Journal of Nuclear Materials 386–388 (2009) 797–800

Contents lists available at ScienceDirect

Journal of Nuclear Materials

journal homepage: www.elsevier.com/locate/jnucmat

Microstructural and thermo-mechanical characterization of carbon/carbon composites

J. Compan, T. Hirai, G. Pintsuk, J. Linke *

IEF2, Forschungszentrum Juelich GmbH, EURATOM-Association, D-52425, Germany

ARTICLE INFO

PACS:
28.52.Fa

ABSTRACT

Since advanced carbon fiber composites for fusion applications, i.e., NB31, its upgraded version NB41 and DMS780, are anisotropic in terms of thermal and mechanical properties, their response under fusion-relevant transient heat loads is highly dependent on the orientation of the material. To understand and predict the material behavior, microstructural investigations as well as tensile tests and thermal conductivity measurements were performed in different directions (along and off the three orthotropic fiber-reinforcement axis). Furthermore, ITER-like disruption loads were applied, in the electron-beam facility JUDITH, on various carbon based materials and their thermal shock response, in terms of weight loss, was compared. Under repeated disruptions, the response of the studied materials is becoming worst if oriented differently than in the direction of highest thermal conductivity and it leads towards more homogeneous but deeper erosion zones with increased tilting angle.

1. Introduction

Lot of experience has been acquired about carbon based materials (CBMs) in nuclear environment over the past decades and their advantages are largely described in literature [1,2]. Carbon/carbon composites are the prime plasma facing materials candidates for the ITER divertor vertical targets. These composites, so-called carbon fiber composites (CFCs) have been developed to improve the thermo-mechanical properties of isotropic fine grain graphite. Nevertheless, under thermal shock loads, e.g., ITER-like disruptions, all CBMs exhibit brittle destruction [3–5]. This phenomenon is due to the intrinsic thermo-mechanical anisotropy of graphitic structures [6,7], the presence of constituents with various structure organization degrees in CBMs (binder and grains) [3] and differently aligned sub-units in CFCs [5,8–10]. Most of the high heat flux tests on candidate CFCs were done only in the direction of their highest thermal conductivity [4], neglecting anisotropical effects. In this study, this lack of experience is addressed by transient high heat flux tests, performed in the electron beam JUDITH, which demonstrate the significant influence of the high anisotropy of the thermal and mechanical properties of CFCs on their response. In addition, thermal conductivity measurements and mechanical tests were performed to generate an expended database for future finite-element calculations to better understand and validate the anisotropic behavior of various CFCs for which several theories have been developed [6,11,12].

2. Material microstructures

One isotropic fine grain graphite was used in this study as basic CBM: R6650 (SGL) [3]. In addition three fusion-relevant CFCs were considered: NB31, its upgraded version NB41 (SNECMA) and DMS780 (DUNLOP) [13]. NB31 and NB41 are both orthotropic (3-directionnal) unbalanced (pitch-PAN (PolyAcryloNitrile)) needled (with PAN fibers) laminates CFCs [5,8,13]. DMS780 is a cross-ply laminates of PAN fibers with a stacking sequence: felt layer (short fibers), fibers at 0°, felt layer, fibers at 90°... Short needling process (from one felt to the consecutive) is also used in DMS780. Polarized light microscopy and SEM imaging of the CFCs allowed to conclude that highly oriented (*c*-axis radial [7]) sheath-like matrix (Fig. 1) was used by the manufacturers to densify the fibrous preforms. In general, carbon fibers present a high thermo-mechanical anisotropy between their transverse and longitudinal axis. In pitch fibers, the higher preferential alignment of larger graphite crystallites along the longitudinal fiber axis leads to a higher thermal conductivity and Young's modulus than for PAN fibers (in their respective longitudinal axis) [6]. The fibers stiffen the composite structure and guide the orientation of the deposited matrix. The role of the matrix is to improve thermal conductivity, to decrease composite porosity and to allow crack deflection under mechanical load [6,11,14,15]. Average densities and volumetric percentage of each relevant sub-unit of the materials are shown in Table 1. The

* Corresponding author. Tel.: +49 2461 61 3230; fax: +49 2461 61 8312.
E-mail address: j.linke@fz-juelich.de (J. Linke).

0022-3115/$ - see front matter © 2009 Elsevier B.V. All rights reserved.
doi:10.1016/j.jnucmat.2008.12.222

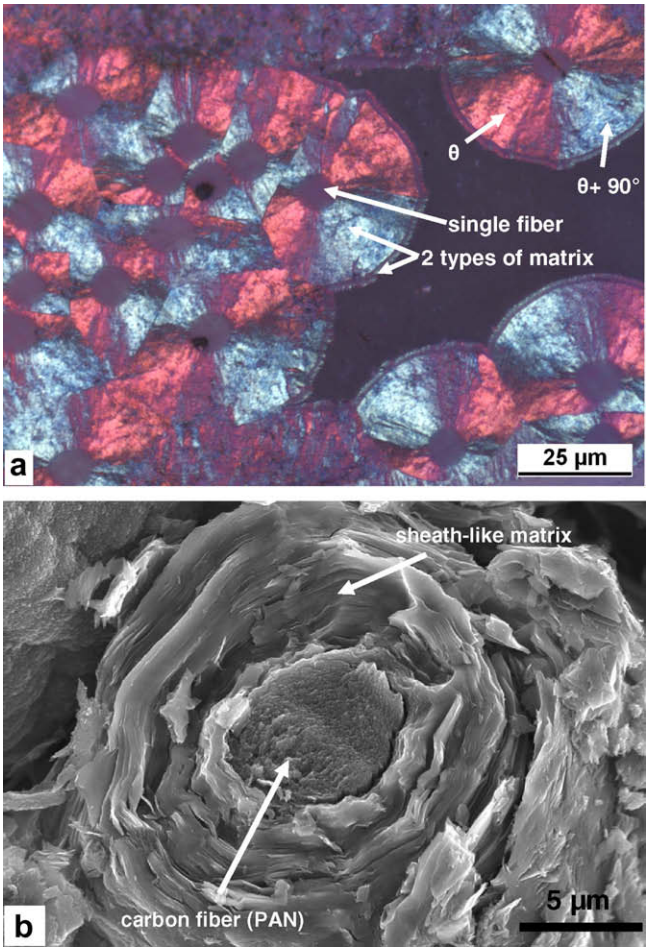

Fig. 1. (a) Polarized light picture of DMS780. Clear Maltese crosses are visible and orthogonally oriented layer planes are highlighted (θ and $\theta + 90°$). (b) SEM micrograph of NB31 (Y) showing sheath-like (*c*-axis radial) matrix and radial PAN fiber. The matrix is elastically bent parallel to the surface of the fiber.

nomenclature of the orthotropic directions is *X*, *Y* and *Z* representing the direction of highest, intermediate and lowest thermal conductivity, respectively.

3. Mechanical testing

Tests of CFCs were performed at room temperature, as it was done extensively for NB31 in [15] since they can retain, or even improve, their mechanical properties until 2000 °C [6,16]. The extracted values are thus considered as lower boundary conditions. In Fig. 2(a), testing results are displayed for the four investigated CBMs in their orthotropic directions. Results of tensile tests of CFCs mainly depend on the type and volumetric content of fibers aligned parallel (or at less than 4–5° [11]) to the loading direction

Table 1
Apparent density and volumetric percentage (values obtained by image analysis of CFCs cross sections) constituting the various CFCs sub-units ((fiber + matrix) in one direction or felt layer). R6650 was input as reference isotropic material.

Material	Density (g cm^{-3})	Porosity (vol.%)	Vol.% *X* direction	Vol.% *Y* direction	Vol.% *Z* direction	Vol.% felt layer
NB31	1.87	8	60	20	12	
NB41	1.94	8	62	18	12	
DMS780	1.81	12.5	23	23	2	40
R6650	1.85	10	90	–		

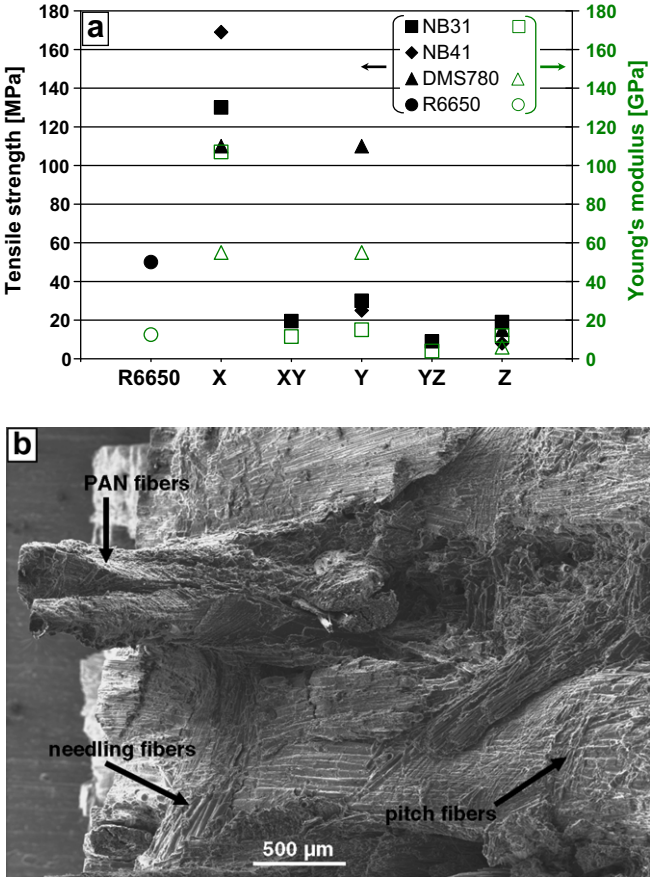

Fig. 2. (a) Averaged room temperature tensile strength and Young's Moduli of various CBMs: NB31, NB41 after [13], DMS780 and R6650 from manufacturers. (b) Top view SEM micrograph of NB31-*XY* fracture surface. Unbroken fiber bundles are visible.

and on the interfacial (fiber/matrix) shear strength. The latter should be low enough to allow crack deflection and significant fiber pull-out [6,11,16]. Only the *X*-directional strength of the tested CFCs (except DMS780 which is balanced in *X* and *Y* direction) is exceeding the one of R6650 as a consequence of the architecture in addition to the low fiber content in the *Y* directions of SNECMA materials and the presence of needling fibers (which is not a continuous reinforcement but done to limit delamination between *X* and *Y* planes) in the *Z* direction. Additional testing of NB31 at 45° off-axis (*XY* and *YZ*) demonstrate that tensile strength as well as young modulus are lower than the ones of the weakest fibrous axis involved (*Y* and *Z*, respectively). These low values are attributed to

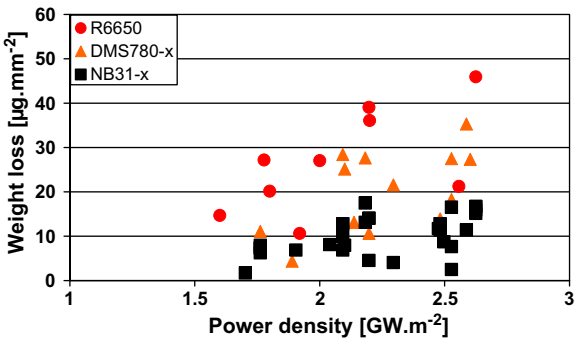

Fig. 3. Weight loss of various CBMs after single ITER-like disruptions loads of 5 ms in their highest thermal conductivity directions.

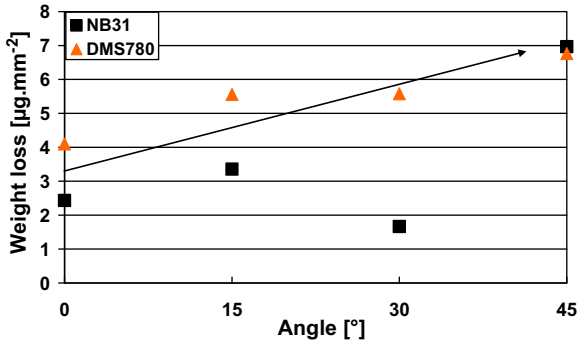

Fig. 4. Average weight loss per shot of NB31 and DMS780 variously oriented after 10 disruptions of 5 ms and 2.6 GW m^{-2} on previously loaded areas. The angle represents the value between the *X* direction and the heat flux direction. Rotation is done in the *XY* plane. The arrow shows the tendency for increasing angle.

shear processes which are maximum between two fiber-reinforcement axis and such tests mostly reflect the properties of the matrix [11,17,18]. The SEM micrograph in Fig. 2(b) illustrates this shear-dominated fracture type. The same behavior is expected for all CFCs.

4. Thermal tests

Various thermal shock specimens were prepared in different orientations as illustrated in [8]. ITER-like disruptions loads [4] were applied in the electron-beam facility JUDITH, using a defined test procedure and different diagnostics [5,8,19]. It was observed that the weight loss per shot, decreases with increasing shot number [5], thus the weight loss during a single disruption can be considered as upper boundary value. Fig. 3 shows the weight loss of various CBMs after 5 ms single disruptions loads. It is clear that graphites exhibit weight losses up to four times higher than NB31, while weight loss of DMS780 is located in an intermediate range. Such tests allow obtaining an experimental criterion for the comparison of the thermal-shock resistance of materials. From [8] it was demonstrated that thermal conductivity is the determinant factor for thermal shock response and that the macroscopic mechanical properties plays a less significant role as the macroscopically weaker CX20002 U (TOYO TANSO) [8,20] shows a similar or even better response than NB31. Additionally, to predict material lifetime, the density of the material (leading to obtain the volume of sacrificed material) should be taken into account

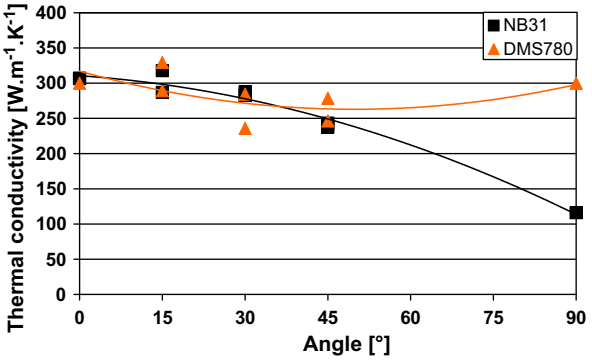

Fig. 5. Angular evolution of the macroscopic thermal conductivity of NB31 and DMS780 (second degree polynomial) between *X* (0°) and *Y* (90°). Rotation was done in the *XY* plane. These values were acquired at room temperature. Discrepancies of thermal conductivity between the 15° and 45° samples decrease to around 10 W m^{-1} K^{-1} at 1200 °C for DMS780 and 50 W m^{-1} K^{-1} for NB31.

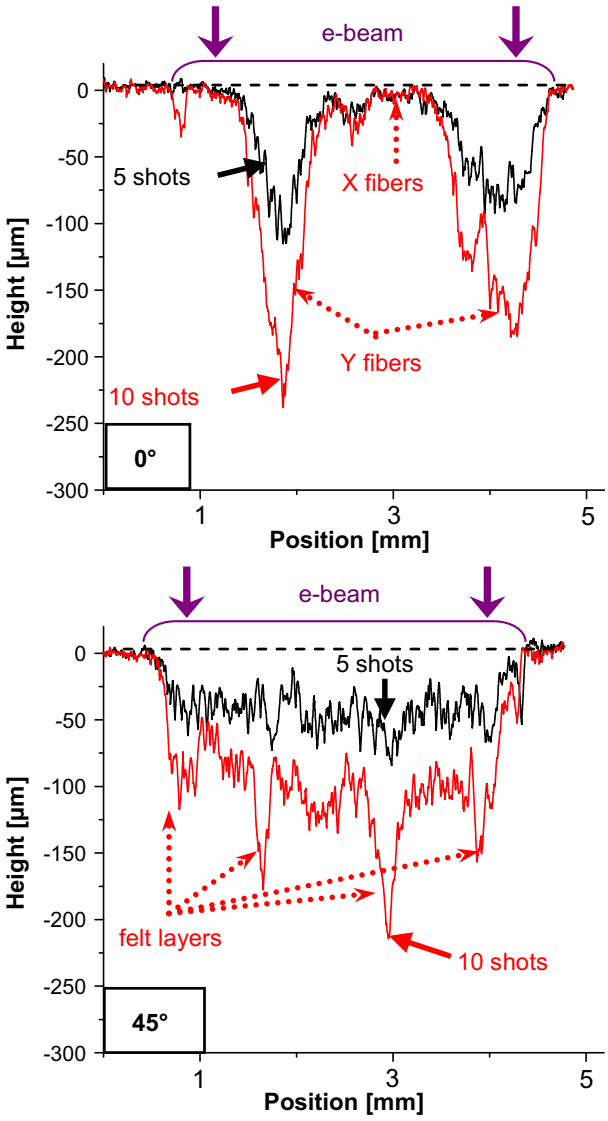

Fig. 6. Surface profiles of DMS780 (0° and 45°) after 5 and 10 disruptions of 5 ms and 2.6 GW m^{-2} on the same positions. The loaded area was 4 × 4 mm^2. Original surface is represented by the dotted line.

in combination with the erosion pattern which is function of the fiber architecture [5]. It was observed [5,8] that tilted NB31 (15°, 30° and 45° (angle between the loading direction and the *X* direction)) lost less weight under single disruptions than NB31 in its original orientation (*X* or 0°).The same behavior was observed for DMS780. It was assumed that tilting the samples would lead to lower temperature differences in between orthogonal fibrous directions (*X* and *Y*) and a better mechanical attachment leading to less ejection of intersected fibers or groups of fibers. But when repeated disruptions on identical positions were applied (Fig. 4), it was observed that weight loss increases with the studied tilting angle. This means that the explanation proposed earlier is only valid for a very limited number of disruptions or for less energetic loadings as used in the current study. The ejection of the hotter fibers (brittle destruction) on the weight loss contribution is high for unloaded CFC surfaces but erosion processes of individual constituents predominates under repeated or high power disruptions. This erosion depends on the macroscopic thermal conductivity, which can be related to the one of the constituents by an electric circuit approximation [21]. This strategy can be applied at the

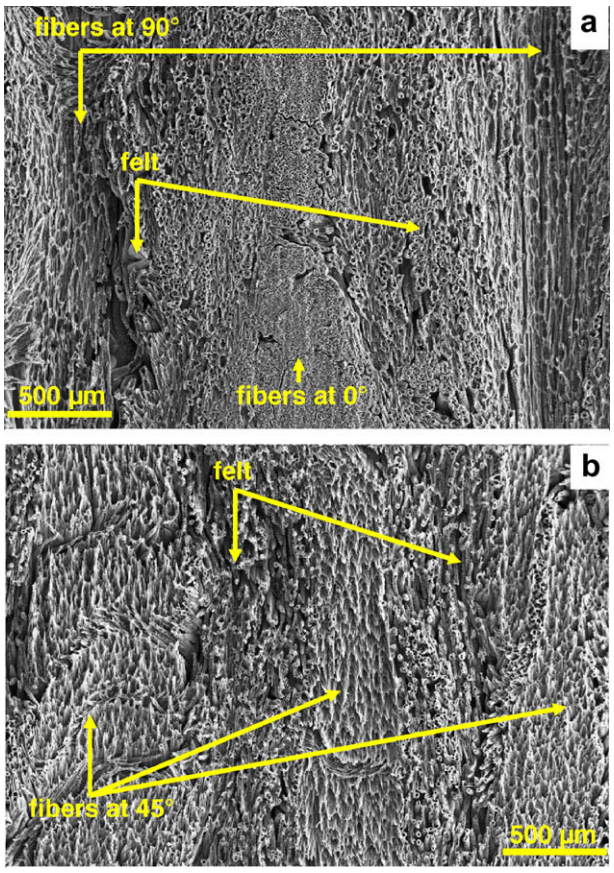

Fig. 7. Top view SEM micrograph of DMS780 after 10 disruptions of 5 ms and 2.6 GW m^{-2}: (a) for the 0° sample and (b) for the 45° sample.

mesoscale (sub-unit scale) and angular variation of thermal conductivity between the long-fiber planes can be assimilated with the evolution of thermal conductivity within a graphite crystal [22,23]. Nevertheless, experimental measurements of the macroscopic thermal conductivity for an angular evolution between *X* and *Y* directions were performed and are plotted in Fig. 5 with the tendencies indicated by solid lines. In Fig. 6 the mechanically acquired surface profiles [5,8] of DMS780 after 5 and 10 identical disruptions are presented. The erosion pattern changes from preferential erosion of fibers aligned perpendicular to the heat flux for the 0° sample, to a more homogeneous and deeper crater for the sample oriented at 45°. The observation of the center of the loaded area of DMS780 (Fig. 7) confirms the information that Fig. 6 are giving. Though, it can be observed that for DMS780 tilted at 45°, the layers which are the most eroded are the felt ones, demonstrating their lower thermal conductivity under this orientation of DMS780 in respect to the two orthogonal laminates (*X* and *Y*). Same behavior was noticed for NB31. Further calculations and experiments must be engaged to determine if, in a fusion divertor configuration, the combination of preferential erosion (creating leading edges constituted of less eroded sub-units) with particles impinging at shallow angles [24] will lead to shorten the lifetime of the CFCs under repeated thermal shocks.

5. Conclusions

CFCs used for fusion are made of highly oriented constituents which are giving rise to very anisotropic thermo-mechanical and thermo-physical properties. CFC architecture, type and treatments of the constituents do allow tailoring thermal and mechanical response; different strategies were used by manufacturers. Off-axis tensile and thermal tests were presented, they allow to better depict the anisotropy of the various CFCs and should be more systematically performed. Ejection of fibers (brittle destruction) during single ITER-like disruption could be limited by appropriate tilting but under repeated high power disruption loads, sublimation seems to be the dominant process of CFC physical erosion. Therefore, under disruption loads impinging perpendicular to the CFC surface, only a high macroscopic thermal conductivity in the direction parallel to a heat flux can help to enhance material lifetime. Nevertheless, the fiber architecture will strongly influence the erosion pattern and its evolution with shot numbers.

Acknowledgements

This work, supported by the European Communities under the contract of Association between EURATOM/FZJ, was carried out within the framework of the European Fusion Development Agreement. The views and opinions expressed herein do not necessarily reflect those of the European Commission.

References

[1] T. Tanabe, Fus. Eng. Des. 81 (2006) 139.
[2] T.D. Burchell, in: T.D. Burchell (Ed.), Carbon Materials for Advanced Technologies, Pergamon, 1999 (Chapter 12).
[3] J. Linke et al., Fus. Eng. Des. 66–68 (2003) 395.
[4] T. Hirai, K. Ezato, P. Majerus, Mater. Trans. 46 (3) (2005) 412.
[5] J. Compan et al., Phys. Scr. T128 (2007) 246.
[6] Peter Morgan (Ed.), Carbon Fibers and their Composites, Taylor and Francis, 2005.
[7] E. Pitzer, W. Hüttner, J. Phys. D: Appl. Phys. 14 (1981) 347.
[8] J. Compan et al., Reduction of thermal shock induced damages in carbon fiber composites, in: Proceedings of the 16th International Conference on Composite Materials (ICCM-16), 2007.
[9] I.S. Landman et al., Phys. Scr. T111 (2004) 206.
[10] S. Pestchanyi, I. Landman, Fus. Eng. Des. 81 (2006) 275.
[11] D. Hull, T.W. Clyne, An Introduction to Composites Materials, 2nd Ed., Cambridge Solid State Science Series, 1996.
[12] C. Sauder, J. Lamon, Carbon 43 (2005) 2044.
[13] A.T. Peacock et al., Phys. Scr. T128 (2007) 23.
[14] H. Hatta et al., J. Compos. Mater. 38 (2004) 1667.
[15] G. Pintsuk et al., Phys. Scr. T128 (2007) 66.
[16] G. Savage, Carbon–Carbon Composites, 1st Ed., Chapman and Hall, 1993.
[17] K.K. Chaulla, Compos. Mater. Sci. Eng, second ed., Springer-Verlag, 1987.
[18] A.K. Kaw, Mechanics of Composite Materials, CRC Press, 1997.
[19] J. Linke et al., J. Nucl. Mater. 283–287 (2000) 1152.
[20] V. Barabash, L.L. Snead, J. Nucl. Mater. 329–333 (2004) 860.
[21] T.R. Guess, B.L. Butler, Optimization of the Thermal Shock Resistance of Carbon–Carbon Composites, vol. 580, ASTM Special Technical Publications, 1975. 229.
[22] B.T. Kelly, Physics of Graphite, Applied Science Publishers, 1981.
[23] A.J. Whittaker, R. Taylor, H. Tawil, Proc. R. Soc. Lond. A 430 (1990) 167.
[24] G. Federici et al., J. Nucl. Mater. 313–316 (2003) 11.